THE JOURNAL OF PHYSICAL CHEMISTRY B

Article

pubs.acs.org/JPCB

Molecular Binoculars: How to Spatially Resolve Environmental Fluctuations by Following Two or More Single-Molecule Spectral Trails at a Time

Vassiliy Lubchenko*,† and Robert J. Silbey‡,§

†Departments of Chemistry and Physics, University of Houston, Houston, Texas 77204-5003, United States

‡Department of Chemistry, Massachusetts Institute of Technology, Cambridge, Massachusetts 02139, United States

ABSTRACT: We propose a novel type of spectral diffusion experiment that enables one to decouple spatial characteristics of the environmental fluctuations, such as their concentration, from the interaction with the chromophore. Traditional hole broadening experiments do not allow for such decoupling in the common case when the chromophore−environment interaction is scale invariant. Here we propose to simultaneously follow the spectral trails of a small number of nearby chromophores—two or more—which thereby sense a highly overlapping set of the fluctuations. To this end, we estimate the combined probability distribution for the frequencies of a set of chromophores contained within the *same* sample. The present setup introduces a new length scale, i.e., the interchromophore distance, which breaks the aforementioned scale invariance and enables one to determine independently the concentration of the environmental fluctuations and their coupling to the chromophores, by monitoring the time after which spectral diffusion of distinct chromophores becomes uncorrelated. We illustrate these results with structural excitations in low temperature glasses.

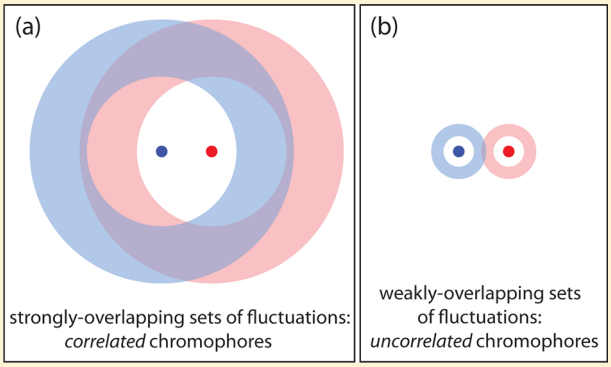

1. INTRODUCTION

Spectral diffusion[1−5] is an indispensable tool for monitoring local motions, in a condensed matter system, that couple to light in a convenient spectral range not directly but through a chromophore. One may monitor the diffusion of the frequencies of either individual chromophores or, more traditionally, a chromophore ensemble, via hole-burning spectroscopy and spin−echo experiments. Single-molecule experiments have provided direct evidence for local fluctuations along with the associated electric-dipole moment and excitation energy, among other things.[6,7] Ensemble measurements, on the other hand, are instrumental in inferring the relaxation spectrum of the local fluctuations and establishing their bulk character, in the first place.

Although heterogeneous in origin, line broadening due to a fluctuating environment often does not follow the usual Gaussian profile. This surprising behavior, elucidated a long time ago by Klauder and Anderson,[4] results when the chromophore−environment interaction is scale invariant, as in the typical case of dipole−dipole interaction A/r^3. Hereby, the line width at an early delay time t is determined by fluctuations situated at large distances $r \sim (\gamma t n)^{-1/3} \gg n^{-1/3}$ (at $t \ll \gamma^{-1}$), where γ and n are the typical relaxation rate and the concentration of the fluctuations, respectively. Because the contributing fluctuations span a distance much larger than the fixed length scales in the problem, such as the typical distance between the fluctuations or size of the chromophore, spectral diffusion is determined by a *combination* of the concentration of the fluctuations and their coupling to the chromophore. In the above A/r^3 example, the hole is Lorentzian with a width that scales linearly with time at early times, $\delta\omega_L \sim \gamma t n|A|$, and reaches at most $\delta\omega_L \sim n|A|$ at long times. Because of such a scale invariance of the chromophore−fluctuation interaction, finite size effects amount to only weak deviations from the Lorentzian hole shape and are difficult to detect on experimentally relevant times.[4,8] As a result, what can be perceived as a remarkable robustness of the Lorentzian hole shape,[4] in fact, imposes a limitation on one's ability to use spectral diffusion to determine the number of environmental fluctuations separately from their coupling to the chromophore.

Here we show this limitation can be circumvented by monitoring simultaneously spectral trails of two or more chromophores. We find that sufficiently fine-scale, frequent spectral jumps are subject to highly overlapping sets of environmental fluctuations and hence are always correlated. In contrast, sufficiently large, rare jumps are largely uncorrelated, if the chromophores are further apart than the typical distance between the fluctuating entities. The decorrelation time scale, on which such uncorrelated jumps begin to appear, directly depends on the concentration of the

Special Issue: Peter G. Wolynes Festschrift

Received: January 30, 2013
Revised: April 8, 2013
Published: April 23, 2013

environmental fluctuations. Thus, using already two chromophores introduces a new length scale in the problem that allows one to determine the distance between the fluctuations. To make an informal analogy, this is not unlike using binocular vision to determine the distance between objects.

An important candidate situation where such experiments can yield crucial information is provided by low temperature glasses. These systems host strongly anharmonic, structural degrees of freedom that dominate the heat capacity and phonon scattering at cryogenic temperatures, often associated empirically with the so-called two-level systems (TLS);[9−11] the nature of the TLS has excited controversy for decades. Lubchenko and Wolynes (LW) have argued[12] these motions—active at low temperatures—are low-barrier relics of the structural configurations responsible for transport in supercooled liquids *above* the glass transition. Their picture leads to quantitative predictions of the cryogenic heat capacity and conductivity,[12,13] Boson peak,[14] negative Grüneisen parameter,[13] the TLS's dipole moment,[15] and, more recently, midgap electronic states in amorphous chalcogenides;[16−18] see reviews in refs 13, 19, and 20. Despite the unified picture advanced by LW's approach, the origin of the two-level systems remains a subject of debate,[21−24] as we have indicated.

The article is organized as follows: First, we recall several results on the spectral diffusion of a single chromophore and delineate the conditions under which distinct chromophores contained within the same sample are correlated. Next, we write down and estimate a correlation function for several chromophores contained within the same sample. We find that, for common types of chromophore−environment coupling, only a small number of chromophores are independent at sufficiently early times. For instance, for the electric dipole−dipole interaction, this number is three. We subsequently estimate the crossover time from this highly correlated regime to complete decorrelation and describe the corresponding changes in the multichromophore correlation function. In the Discussion section, we use these results to propose a novel experiment whereby the correlated spectral trails of two or more chromophores can be used to establish the concentration of the entities responsible for environmental fluctuations. We describe expected results for a specific system of interest, i.e., low temperature glasses. Finally, these results can be employed to discuss ensemble averaging issues in hole-burning experiments. We show that, under most circumstances, this averaging is indeed adequate.

2. ORIGIN OF INTERCHROMOPHORE CORRELATIONS

We set up the spectral diffusion problem in a standard fashion[1−5] (see also our earlier work[8]): The precise value of the transition frequency of chromophore α at time t is determined by the current configuration of the environmental degrees of freedom, which we model as distributed two-level systems (TLS), or "spins" $\sigma_j = \pm 1$, according to

$$\omega_\alpha(t) = \omega_{\alpha,\mathrm{mp}} + \sum_j J_{\alpha j}\sigma_j(t) \tag{1}$$

where $J_{\alpha j}$'s are some coupling constants that are generically larger for nearby spins and $\omega_{\alpha,\mathrm{mp}}$ is the center of the inhomogeneous band of chromophore α. Throughout the article, we will use Greek indices to label chromophores and Latin symbols to label distinct spins. We will not consider the effects of distributed central frequencies, $\omega_{\alpha,\mathrm{mp}}$; see ref 8. One may then set $\omega_{\alpha,\mathrm{mp}} = 0$ for convenience. The spins are assumed to flip independently of each other and of the chromophores. (Effects of correlation between spin locations can be accounted for as in ref 8; effects of interaction between the spins have been treated in ref 25; see also below.) We will assume for concreteness that state +1 (or simply +) of each two-level system is the higher energy state: $E_{i,+} - E_{i,-} = E_i \geq 0$. We will further assume that each two-level system relaxes exponentially so that the waiting time distribution to jump from state (+) to state (−) is $\psi_{(-)\leftarrow(+)}(t) = \gamma_+ e^{-\gamma_+ t}$ and *vice versa* $\psi_{(+)\leftarrow(-)}(t) = \gamma_- e^{-\gamma_- t}$, where $\gamma_{i,-}/\gamma_{i,+} = e^{-\beta E_i}$ by the detailed balance.

Two *a priori* distinct distribution functions for the time-dependent value of the chromophore frequency can be written down. One yields the likelihood of observing the line at a frequency ω at time t, subject to the distribution of time traces of the environmental spins:

$$\rho_\alpha(\omega, t) = \langle \delta[\omega - \sum_j J_{\alpha j}\sigma_j(t)]\rangle_t = \int \frac{d\xi}{2\pi} e^{i\xi\omega}\langle e^{-i\xi\sum_j J_{\alpha j}\sigma_j(t)}\rangle_t \tag{2}$$

where the angular brackets denote the time-trace averaging. Alternatively, one may compute an ensemble averaged value of the chromophore frequencies, as pertinent to hole burning experiments. The hole will broaden according to the following expression:

$$\rho(\omega, t) = \int \frac{d\xi}{2\pi} e^{i\xi\omega}\langle\langle e^{-i\xi\sum_j J_{\alpha j}\sigma_j(t)}\rangle\rangle_\alpha \tag{3}$$

where the double angular brackets $\langle\langle ... \rangle\rangle_\alpha$ denote averaging with respect to the distinct chromophores not fluorescing at time t.

While hole burning experiments yield an ensemble-averaged quantity related to the distribution function from eq 3, it is the time-averaged quantity from eq 2 and its likes that are computed in practice. The present authors have shown[8] that, apart from the overall drift of the spectral hole, its evolution is given by the expression

$$\rho_\alpha(\omega, t) = \int \frac{d\xi}{2\pi} e^{i\xi\omega + \sum_j B_j(\xi J_{\alpha j}, t)} \tag{4}$$

where

$$B_j(\xi J_{\alpha j}, t) \equiv \frac{1}{2}\ln[\cos^2(\xi J_{\alpha j}) + f_j^2 \sin^2(\xi J_{\alpha j})] \tag{5}$$

$$f_j \equiv f_j(t, \sigma_{j0}) \equiv \frac{1}{\gamma_j}[\gamma_{j,\sigma_{j0}}(2e^{-\gamma_j t} - 1) + \gamma_{j,-\sigma_{j0}}] \tag{6}$$

and

$$\gamma_j \equiv \gamma_{j,+} + \gamma_{j,-} \tag{7}$$

The quantity $\sigma_{j0} \equiv \sigma_j(0)$ stands for the initial value of spin j. In practice, one should assume a particular distribution of the initial values of the spins, which is not necessarily equilibrium and, even if equilibrated, it may have been manipulated, for instance, by a polarizing field. The aforementioned drift of the spectral hole occurs when the hole is burned sufficiently away from the most probable value of the chromophore frequency. The resulting effects have been already analyzed[8] and will not concern us here. On the other hand, the sum $\sum_j B_j$ in eq 4

dx.doi.org/10.1021/jp401085p | J. Phys. Chem. B 2013, 117, 12734−12741

reflects the main contribution to the line broadening proper and will be considered in what follows.

In the rest of the article, we will assume, for concreteness, the chromophore−spin interaction is (electric) dipole−dipole:

$$J_{\alpha j} = \frac{(\mathbf{g}_\alpha \mathbf{g}_j) - 3(\mathbf{g}_\alpha \mathbf{e}_{\alpha j})(\mathbf{g}_j \mathbf{e}_{\alpha j})}{r_{\alpha j}^{\ 3}} \tag{8}$$

where $\mathbf{e}_{\alpha j} \equiv \mathbf{r}_{\alpha j}/r_{\alpha j}$. Note that a *phonon*-mediated chromophore−spin interaction is, in general, of more complicated, tensorial form. This complication can be addressed in a standard fashion; see ref 26 and also below.

The underlying assumption behind equating the quantities from eqs 2 and 3 is, superficially, that the time and ensemble averages are equivalent. And indeed, the two quantities should be equal, if distinct chromophores are completely uncorrelated, which would be strictly true if the chromophores were placed in distinct similar samples or were infinitely diluted. However, in an actual sample, the spectral jumps of distinct chromophores are subject to overlapping sets of spins, and especially so at short observation times or early stages of hole growth. To see this, we use the result from ref 8 that, to a good approximation, the "broadening" kernel from eq 4, for not too small ξ, is given by the expression

$$\sum_j B_j(\xi J_j, t) \simeq -\delta\omega_L|\xi| \tag{9}$$

where

$$\delta\omega_L = \frac{2\pi^2}{3} A\langle n(1 - |f_j|)\rangle \tag{10}$$

The coupling constant is $A = g_\alpha g_j[1 + \ln(\sqrt{3} + 2)/2\sqrt{3}]/2$ (see Appendix B of ref 8), and it reflects angular averaging over the orientation of the TLS's dipole moments. The angular brackets in eq 10 signify averaging over distinct spins. The concentration n is kept inside the angular brackets to include situations in which the parameters of the TLS are distributed. Under these circumstances, the partial quantities of spins with distinct energy splittings or relaxation rates may not be the same. Note that in obtaining expressions 9 and 10, no "annealed" averaging with respect to spin locations was performed, similarly to the procedure of Klauder and Anderson[4] and in contrast with many other common approaches;[1−3] see ref 8 for a detailed discussion.

The linear scaling of the diffusion kernel $\sum_j B_j(\xi J_j, t)$ with $|\xi|$ results because, not too close to the edges of the spectral hole, the bulk contribution to the sum $\sum_j B_j(\xi J_j, t) \propto \int d^3\mathbf{r} B(\xi A/r^3, t)$ is determined by the largest length scale in the problem, i.e., $|\xi A|^{1/3}$, as elucidated by Klauder and Anderson.[4] One may think of the spins that dominate the sum as located within a spherical shell of a thickness proportional to the radius itself; see illustration in Figure 1. The linear scaling with $|\xi|$ implies the spectral hole is a Lorentzian with a (time-dependent) width given by the parameter $\delta\omega_L$ from eq 10. Other length scales in the problem, such as due to spin−spin correlations or chromophore size, contribute to chromophore-specific deviations from the aforementioned bulk term and result in corrections to the linear scaling in eq 9; see a detailed discussion in ref 8. In the simplest example, $\sum_j B_j(\xi J_j, t) \propto -\xi^2$ for the smallest values of ξ, resulting in ultimately Gaussian tails of the line shape.[4,8]

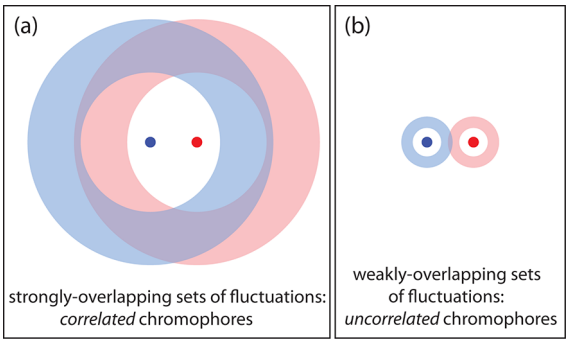

Figure 1. The two small, filled circles, in each panel, denote two chromophores. The thick shells indicate locations of the environmental fluctuations that dominate the spectral diffusion kernel $\sum_j B_j(\xi J_j, t)$ at a given time t, for the chromophore located at the center of a shell. Both the radius and thickness of a shell are set by the length scale $|\xi A|^{1/3}$ in the common case when the chromophore−TLS interaction is dipole−dipole $\propto A/r^3$. Panels a and b illustrate situations where the sets of fluctuations for two chromophors overlap significantly and weakly, respectively. The former case can always be realized at early enough time t (i.e., for sufficiently high-frequency spectral jumps), while the latter situation can take place only when the chromophores are further apart than the typical spacing between the fluctuating entities; see eqs 19 and 20.

Regardless of the detailed shape of the distribution $\rho_\alpha(\omega, t)$ from eq 4, the *width* of $\rho_\alpha(\omega, t)$ is determined mainly by the values of $\xi \sim \xi_*$ such that $|\sum_j B_j(\xi J_j, t)| \simeq 1$, implying, by eqs 9 and 10, that $|\langle(1 - |f_j|)n\rangle A\xi_*| \sim 1$. On the other hand, the sum over the spins in eq 4 is dominated by spins located at chromophore−TLS distance: $r \sim |\xi_* A|^{1/3}$, because this is the only relevant length scale at short time scales,[8] as already mentioned. Consequently,

$$r \sim \langle(1 - |f_j|)n\rangle^{-1/3} \tag{11}$$

Since at early times, $1 - |f_j| \simeq 2\gamma_{j,\pm}t$, the fine-scale, high-frequency spectral jumps, which correspond to early evolution of a burned hole, are dominated by spins located at large distances

$$r \sim (\langle n\gamma\rangle t)^{-1/3}, \quad (t \ll \gamma^{-1}) \tag{12}$$

as mentioned in the Introduction. We thus observe that, at sufficiently short times, even very remote chromophores are subject to fluctuations from highly overlapping sets of environmental degrees of freedom, as in Figure 1a, and thus the dynamics of distinct chromophores are correlated.

3. EVALUATION OF MULTICHROMOPHORE CORRELATIONS

To assess the magnitude of chromophore−chromophore dynamical correlation stemming from the overlap of the respective sets of environmental fluctuations, here we set out to estimate the following distribution function for the frequencies of an arbitrary number (m) of chromophores contained within the *same* sample:

$$\rho^{(m)}(\{\omega_\alpha\}, t) = \int\left(\prod_\alpha^m \frac{d\xi_\alpha}{2\pi}\right) e^{i\sum_\alpha^m \xi_\alpha\omega_\alpha}\left\langle e^{-i\sum_\alpha^m \xi_\alpha \sum_j J_{\alpha j}\sigma_j(t)}\right\rangle_t \tag{13}$$

This quantity is an obvious generalization of the single-chromophore frequency distribution function from eq 2. It is

dx.doi.org/10.1021/jp401085p | J. Phys. Chem. B 2013, 117, 12734−12741

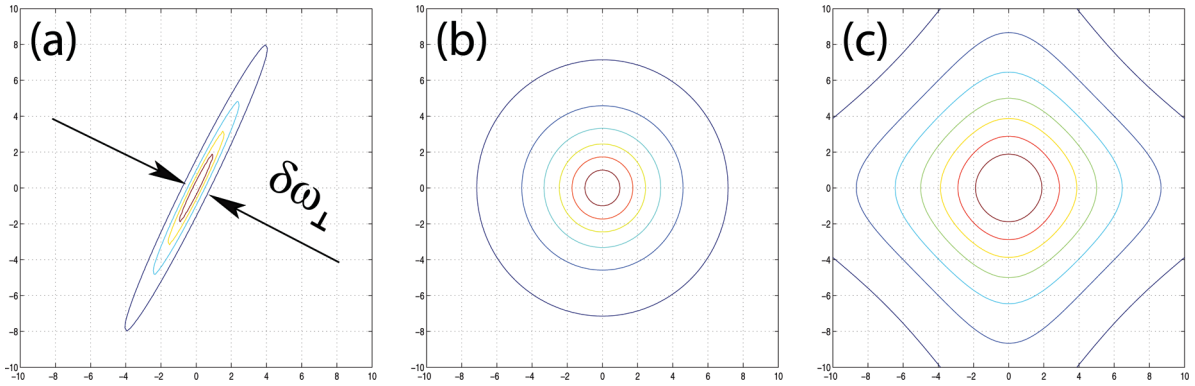

Figure 2. Contour plots of the two chromophore correlation function $\rho^{(2)}(\omega_1, \omega_2)$ at some arbitrary time: (a) correlated case of nearly parallel chromophores: $\mathbf{g}_1 = (1, 0.2, 0)$, $\mathbf{g}_2 = (2, 0, 0)$; (b) correlated case of perpendicular dipoles: $(\mathbf{g}_1\mathbf{g}_2) = 0$; (c) uncorrelated case $\rho^{(2)}(\omega_1, \omega_2) = \rho^{(1)}(\omega_1)\rho^{(1)}(\omega_2)$. The horizontal and vertical axes in each panel correspond to ω_1 and ω_2, respectively.

also a correlation function in that it allows one to monitor conditional probabilities of the individual chromophore frequencies. Note that the angular-bracketed expression, as a function of $\{\xi_\alpha\}$, is the generating function of the $\rho^{(m)}(\{\omega_\alpha\}, t)$ distribution.

By the same logic that led to eq 4, we can conclude that

$$\langle e^{-i\sum_\alpha^m \xi_\alpha \sum_j J_{\alpha j}\sigma_j(t)}\rangle_t = e^{\sum_j B_j(\sum_\alpha J_{\alpha j}\xi_\alpha)} \equiv e^{B^{(m)}(\{\xi_\alpha\})} \tag{14}$$

with B_j from eq 5. This expression appears quite difficult to compute at arbitrary times. In a somewhat formal exercise, let us begin, however, with computing the small ξ asymptotics of eq 14, which is straightforward at arbitrary values of time t. These asymptotics determine the extent of the (ultimately) Gaussian tails of the spectral hole and are relevant only for very large chromophores and/or high spin concentrations.[8] Using eqs 5 and 14, expanding to the second order in ξ, replacing $\sum_j \to n\int d^3\mathbf{r}_j$, and averaging with respect to the orientation of g_j results in a quadratic form for the broadening kernel:

$$B^{(m)}(\{\xi_\alpha\}) \underset{\xi_\alpha\to 0}{\longrightarrow} -\sum_\alpha \frac{\delta\omega_{G,\alpha}{}^2 \xi_\alpha{}^2}{2} - \frac{4\pi}{3}\langle n g_j{}^2(1 - f_j{}^2)\rangle \sum_{\alpha<\beta}^m J_{\alpha\beta}\xi_\alpha\xi_\beta \tag{15}$$

where the width parameter, $\delta\omega_{G,\alpha}{}^2 = (27\pi/9R_\alpha{}^3)g_\alpha{}^2\langle n g_j{}^2(1 - f_j{}^2)\rangle$, corresponds to the very tails of the line shape of individual chromophore α and R_α is the radius of the chromophore molecule. The effective chromophore−chromophore "coupling" $J_{\alpha\beta} = [\mathbf{g}_\alpha\mathbf{g}_\beta - 3(\mathbf{g}_\alpha\mathbf{e}_{\alpha\beta})(\mathbf{g}_\beta\mathbf{e}_{\alpha\beta})]r_{\alpha\beta}^{-3}$ turns out to be simply the dipole−dipole interaction between chromophores α and β. In obtaining eq 15, we assumed the chromophores are significantly smaller than their mutual separation. Note also that it is easier to perform the $\mathbf{r}_j$ integration in the cross-terms by first presenting the $J_{\alpha j}$ coupling via their Fourier transform. Now, we observe that the magnitude of the "inter-chromophore couplings" $J_{\alpha\beta}$ in eq 15 is scaled down relative to the diagonal pieces roughly by a factor of $(R/r_{\alpha\beta})^3$, where R is the generic chromophore size. Therefore, correlations in the Gaussian tails are predicted to be barely noticeable, unless the chosen chromophores happen to be nearly on top of each other.

Fortunately, the situation is much more interesting for the more experimentally relevant central portions of the correlation function $\rho^{(m)}(\{\omega_\alpha\}, t)$. Consider a set of chromophores occupying a compact region significantly smaller than the sample dimensions. At the earliest times, by eq 12, a large r shell dominates the sum over the environmental spins, enabling one to make an approximation $\sum_\alpha J_{\alpha j}\xi_\alpha \simeq (\sum_\alpha \mathbf{g}_\alpha\xi_\alpha)[\mathbf{g}_j - 3\mathbf{e}_j(\mathbf{g}_j\mathbf{e}_j)]/r_j^3$, where the radius-vector $\mathbf{r}_j$ points generically from the middle of the chromophore cluster. In this limit, corresponding to the lowest order term in a multipole expansion, the multichromophore broadening kernel reduces to the single-chromophore kernel for a chromophore with dipole moment $\mathbf{g}$ but with the replacement $|\mathbf{g}\xi| \to |\sum_\alpha \mathbf{g}_\alpha\xi_\alpha|$:

$$\rho^{(m)}(\{\omega_\alpha\}) \underset{t\to 0}{\longrightarrow} \int\left(\prod_\alpha^m \frac{d\xi_\alpha}{2\pi}\right) e^{i\sum_\alpha^m \xi_\alpha\omega_\alpha - \delta\omega_L|\sum_\alpha \mathbf{g}_\alpha\xi_\alpha|/g_0} \tag{16}$$

where $\delta\omega_L$ is the width of the spectral hole of an isolated chromophore with dipole moment $\mathbf{g}_0$, as in eq 10. Here, the coupling constant is $A = g_0 g_j[1 + \ln(\sqrt{3} + 2)/2\sqrt{3}]/2$.

Before computing the multidimensional integral in eq 16, it is beneficial to first assess some of the general properties of the resulting correlation function. One may transform the integral identically by multiplying it by $1 = \int(d^3\boldsymbol{\zeta}d^3\boldsymbol{\eta}/(2\pi)^3)e^{i\boldsymbol{\zeta}\boldsymbol{\eta}}$ and simultaneously replacing $\sum_\alpha \mathbf{g}_\alpha\xi_\alpha$ by $\boldsymbol{\zeta} + \sum_\alpha \mathbf{g}_\alpha\xi_\alpha$. Next, change variables, $\boldsymbol{\zeta}' = \boldsymbol{\zeta} + \sum_\alpha \mathbf{g}_\alpha\xi_\alpha$, $\xi_\alpha' = \xi_\alpha$, and perform the integration over all ξ_α's. The result of these manipulations is the following formal expression:

$$\rho^{(m)}(\{\omega_\alpha\}) \underset{t\to 0}{\longrightarrow} \int \frac{d^3\boldsymbol{\zeta}d^3\boldsymbol{\eta}}{(2\pi)^3} e^{i\boldsymbol{\zeta}\boldsymbol{\eta} - \delta\omega_L|\boldsymbol{\zeta}|/g_0} \prod_\alpha^m \delta[\omega_\alpha - \mathbf{g}_\alpha\boldsymbol{\eta}] \tag{17}$$

The product of the δ-functions in eq 17 elucidates a peculiar correlation that takes place between the chromophores at very early times. Since at most three $\mathbf{g}_\alpha$ vectors can be linearly independent, the rest of the $\mathbf{g}_\alpha$ vectors are linear combinations of those chosen three. As a result, only up to three chromophore frequencies can be regarded as not fully correlated random variables, while the rest of the frequencies are linear combinations of those chosen three, according to eq 17. These conclusions are hardly surprising, since the chromophores, again, are all subject to the very same set of environmental degrees of freedom at early enough times. Note that in a common case of *tensorial* chromophore−spin coupling the statements above need to be revised. Here, the number of independent chromophores cannot exceed six, the latter being the number of independent variables needed to specify the force field due to a chromophore/spin.

dx.doi.org/10.1021/jp401085p | J. Phys. Chem. B 2013, 117, 12734−12741

Let us consider in more detail the important case of two chromophores: $\alpha = 1, 2$. At the short times in question, eq 9 holds. It is straightforward to show, using either eq 16 or 17, that

$$\rho^{(2)}(\omega_1, \omega_2) \xrightarrow[t\to 0]{} \frac{(1/2\pi)\delta\omega_L|\mathbf{g}_1 \times \mathbf{g}_2|^2 {g_0}^2}{[\delta\omega_L{}^2|\mathbf{g}_1 \times \mathbf{g}_2|^2 + {g_0}^2(\mathbf{g}_2\omega_1 - \mathbf{g}_1\omega_2)^2]^{3/2}} \quad (18)$$

The correlation described by eq 18 will be most conspicuous when $\mathbf{g}_1$ and $\mathbf{g}_2$ are strictly parallel, in which case $\rho^{(2)}(\omega_1, \omega_2; t)$ is a thin ridge along the $g_2\omega_1 - g_1\omega_2 = 0$ line. Viewed sideways, the ridge is a bell-shaped curve, which is close to a Lorentzian of infinite height in the strict limit $|\mathbf{g}_1 \times \mathbf{g}_2| \to 0$. (This is easiest to see by substituting $\mathbf{g}_1 \| \mathbf{g}_2$ directly into eq 16 and integrating over ξ_1 and ξ_2, which yields $\rho^{(2)}(\omega_1, \omega_2) = \rho^{(1)}(\omega_1)\delta(\omega_2 - \omega_1 g_2/g_1)$, where $\rho^{(1)}(\omega_1)$ is the Lorentzian spectral hole corresponding to an isolated chromophore 1.) Note that the shape of the actual correlation function is never strictly Lorentzian because of the "multipole" effects; see below.

Generally, the contour plots of the $\rho^{(2)}(\omega_1, \omega_2)$ function from eq 18 are ellipsoids. For instance, the case of strictly perpendicular chromophores yields a correlation function $\rho^{(2)}(\omega_1, \omega_2; t) \propto [\delta\omega_L + {\omega_1}^2 + {\omega_2}^2]^{-3/2}$, where we have rescaled ω's by the corresponding g's. While less pronounced than in the collinear case, the correlation is still detectable, as is clear from comparison with the uncorrelated function, which is the product of the one-particle distribution functions: $\rho^{(1)}(\omega_1)\times\rho^{(1)}(\omega_2) = (\delta\omega_L/\pi)^2(\delta\omega_L{}^2 + {\omega_1}^2)^{-1}(\delta\omega_L{}^2 + {\omega_2}^2)^{-1}$. The mentioned patterns of correlation (or lack thereof) are demonstrated in Figure 2.

The uncorrelated form from Figure 2c actually gives the long-time limit of the two-chromophore correlation function, albeit *only* if the chromophores are sufficiently far apart. How far? The crossover to this long time behavior takes place when the size of the shells contributing to the spectral diffusion of the two chromophores becomes comparable to the distance between the chromophores; see Figure 1. Combining eq 11 with $r \sim r_{12}$ shows the crossover will occur roughly at time t_{cr} such that

$$\langle n[1 - |f_j(t_{cr})|]\rangle(r_{12}/2)^3 \sim 1 \quad (19)$$

which is possible only if

$$(r_{12}/2)^3 > 1/n \quad (20)$$

because $|f_j| \le 1$ and, hence, $\langle |A|n(1 - |f|)\rangle < \langle |A|n\rangle$. Despite the qualitative nature of the criterion in eq 19, we have kept the factor of one-half at r_{12} because it corresponds to almost an order of magnitude when cubed.

It is the condition in eq 20 that needs to be satisfied for two chromophores to eventually decorrelate. To rephrase the result in eqs 19 and 20 in simple terms, if two chromophores are located at a distance exceeding the typical separation of environmental fluctuations, the chromophores will first undergo highly correlated spectral diffusion but will eventually experience rare, large-magnitude spectral jumps that are uncorrelated. These large-magnitude jumps stem from non-overlapping subsets of the fluctuations that are significantly closer to one of the chromophores than the other.

Equation 18 applies quantitatively, largely, until the decoupling occurs. Conversely, the time window of poor applicability of eq 18 will be narrow, for the following reasons: We have seen in ref 8 that the crossover region between the large ξ, linear and small ξ, quadratic asymptotics of the broadening kernel $B(\xi)$ is narrow. Hereby, the corrections to the strict $|\xi|$ asymptotics become significant only in the crossover region itself, implying the simple result from eq 19 is semi-*quantitative*. Consistent with this conclusion, the "multipole" corrections to eq 16 scale slower than the linear time dependence of the leading term, as discussed in the Appendix.

Particularly interesting is the case of precisely collinear chromophores: $\mathbf{g}_1 \| \mathbf{g}_2$. Here, the linear in t component of the ridge thickness, $\delta\omega_\perp$ in Figure 2a, is identically zero in the lowest order expansion from eq 16. ($\delta\omega_\perp$ is measured along the $g_1\omega_1 + g_2\omega_2 = 0$ line, in the $|\mathbf{g}_1 \times \mathbf{g}_2| \to 0$ limit.) We show in the Appendix that the distribution's profile along the "perpendicular" direction is weakly non-Lorentzian with the width given roughly by

$$\delta\omega_\perp(t) \sim |A|r_{12}(n\langle\gamma\rangle t)^{4/3} \quad (21)$$

Consistent with $\delta\omega_\perp$ vanishing in the lowest order, monopole approximation, the line width scales superlinearly with time at early times, $\gamma t \ll 1$.

The case of three chromophores can be worked out similarly to the two-chromophore case above; we provide the results in the Appendix for the reader's reference. The "contour lines" of the chromophore−chromophore correlation function are now ellipsoids whose shape and orientation depends on the mutual orientation of the dipole moments of the chromophores.

4. DISCUSSION

The formal findings described above can be summarized as follows: We have evaluated, approximately, the probability distribution for the frequencies of several chromophores contained within the same sample and hence coupled to the very same set of fluctuating environmental degrees of freedom. We have established that on sufficiently short time scales, the spectral trails of even remote chromophores are highly correlated. In contrast, sufficiently large, rare spectral jumps of the chromophores are decorrelated but *only* if the distance between the chromophores exceeds the typical spacing between the environmental fluctuations. Furthermore, if the former sufficiently exceeds the latter—so that $\langle\gamma\rangle t_{cr} \ll 1$—the expression (eq 19) for the crossover time simplifies:

$$t_{cr} \sim [(r_{12}/2)^3\langle n\gamma\rangle]^{-1}, \quad (t_{cr} \ll \langle\gamma\rangle^{-1}) \quad (22)$$

where, note, the condition from eq 20 is satisfied automatically. In contrast with regular spectral diffusion experiments, here the concentration of the environmental fluctuations enters in a measurable quantity *separately* from the coupling strength between the chromophores and the fluctuations. Thus, with the knowledge of the distance between the chromophores and the relaxation time of the fluctuations, which can be determined independently, eq 19 or 22 can be used to establish the concentration of environmental fluctuations, by detecting the typical decorrelation time between two or more chromophores. (The relaxation time of the fluctuations can be measured using hole burning, for instance.)

On the basis of these findings, we suggest the following, two-chromophore correlation experiment. Choose a cutoff time t. Record instantaneous values of the frequencies of two chromophores between time 0 and time t and plot them against each other. Alternatively, one may create a 2D histogram of ω_1, ω_2 pairs. Shift the "center of mass" of the

plot and the histogram to the origin. Repeat the above procedure—while adding new points to the same plot and histogram—until the histogram becomes sufficiently smooth. In practice, one may use very long spectral trails and extract distinct, possibly overlapping portions of length t from the trails, while shifting the centers of mass to the origin for individual portions. The following results are expected, depending on the value of t: For t sufficiently short, the "cloud" on the (ω_1, ω_2) plot or contour plots of the histogram should have an ellipsoidal shape, similarly to Figure 2a and b. The shape of the histogram itself will not be precisely as given by eq 18 because the latter equation gives the correlation between two frequencies at a certain time scale. In contrast, the experiment we have just described also includes a *superposition* of histograms from Figure 2a and b at times between 0 and t. Nevertheless, although the overall width of the $\rho^{(2)}(\omega_1, \omega_2)$ surface depends on time, the shape of its cross sections does not. Thus, we expect that the contour plots for sufficiently short delay times t will be similar to those in Figure 2a or b. Now, as the time t exceeds a certain crossover time t_{cr}—given the chromophores are not too close to each other—the contour plots should develop portions with negative curvature characteristic of uncorrelated chromophores, as in Figure 2c. Note that, sufficiently far away from the origin, the contour plots in the uncorrelated case become hyperbolas: $\omega_1 \propto 1/\omega_2$. Given the crossover time determined in this way, the known distance between the chromophores, and the typical relaxation rate of the fluctuating environmental degrees of freedom, one can estimate the concentration of the fluctuations, according to eq 22, if t_{cr} is shorter than γ^{-1}, or the more general eq 19.

Let us illustrate the above proposal using structural glasses as an example, where, at very low temperatures, the environmental degrees of freedom are well approximated by two-level systems (TLS).[12−14] At $T = 0.1$ K or so, the most likely relaxation time of a TLS is about a millisecond, while the relaxation spectrum is effectively unbounded; see refs 13 and 27 and references therein. In view of the nearly flat spectrum of the TLS and denoting the corresponding spectral/spatial density of states with $\bar{P}$, we obtain the concentration of thermally active two-level systems is given approximately by[12] $n \simeq \bar{P}T \simeq T/T_g\xi^3 \sim 10^{16}$ cm^{-3}. Here, T_g is the glass transition temperature and ξ is the cooperativity size of the liquid at the glass transition, which is 2−4 nm depending on the substance.[28] According to eq 22, two chromophores placed at a distance $r_{12} \gg \xi(T_g/T)^{1/3} \sim \xi\cdot 10^1$ will eventually decorrelate. For instance, for $r_{12} \simeq 200$ nm $\simeq 10^2\xi$, the crossover time is about one tenth of a millisecond, at a temperature of 0.1 K or so. In the above argument, we have assumed that the fastest two-level systems dominate the $\langle n\gamma\rangle$ average. Despite the enormously broad distribution of relaxation times in low T glasses, this assumption is indeed valid, as we show by an explicit calculation in the Appendix. Implementing the present experiment in cryogenic glasses poses challenges in that it requires very low temperatures and, at the same time, monitoring the spectral trails with a rather high time resolution. Because of the fast dependence of the relaxation time of a TLS on temperature, namely, $1/T^3$,[13,29] raising the temperature by a factor of 10 would require enhancing the time resolution by 3 orders of magnitude.

Finally, in view of the tight correlation between even very remote chromophores, on sufficiently short time scales, we need to comment on the validity of ensemble averaging in hole burning experiments. According to eq 12, at times shorter than γ^{-1}/L^3n, where L gives the sample dimensions, the frequencies of all chromophores will be changing synchronously. Under these circumstances, the spectral hole would not broaden but, instead, jump around. (Here, we neglect the effects of retardation for the chromophore−TLS interaction, which could be significant, if the coupling is elastic.) The width of the hole would be given by eq 21 and thus would indeed vanish at short times faster than the typical magnitude of the jumps of individual chromophores. Conversely, consistent with the expected ergodicity of large enough samples, the coefficient at the superlinear, $t^{4/3}$ term diverges in the infinite sample limit $r_{12} \to \infty$. Such lack of ensemble averaging in hole-burning experiments at early times would be very difficult to observe, however. Again, using cryogenic glass as an example, we observe that, for a sample of size 1 cm across, ensemble averaging will always be adequate because of the smallness of the factor $1/L^3n \sim 10^{-16}$.

APPENDIX: AUXILIARY RESULTS

Three Chromophores in the Short-Time ("Monopole") Limit. Equation 17 can be used to show that the three-chromophore correlation function is given by the following expression in the short time limit:

$$\rho^{(3)}(\omega_1, \omega_2, \omega_3) \underset{t\to 0}{\longrightarrow} \frac{(1/\pi^2)\delta\omega_L{}^3[\mathbf{g}_1, \mathbf{g}_2, \mathbf{g}_3]^3\mathbf{g}_0{}^3}{\{\delta\omega_L{}^2[\mathbf{g}_1, \mathbf{g}_2, \mathbf{g}_3]^2 + g_0{}^2([\boldsymbol{\omega}, \mathbf{g}_1, \mathbf{g}_2]^2 + [\boldsymbol{\omega}, \mathbf{g}_2, \mathbf{g}_3]^2 + [\boldsymbol{\omega}, \mathbf{g}_1, \mathbf{g}_3]^2)\}^2} \tag{23}$$

where $\boldsymbol{\omega} \equiv (\omega_1, \omega_2, \omega_3)$ is a 3D vector made up of the frequencies of the three chromophores and the triple product of three vectors $\mathbf{a}_1$, $\mathbf{a}_2$, and $\mathbf{a}_3$ is defined in the usual way: $[\mathbf{a}_1, \mathbf{a}_2, \mathbf{a}_3] \equiv (\mathbf{a}_1\cdot[\mathbf{a}_2 \times \mathbf{a}_3])$.

Equation 23 explicitly demonstrates what we have already seen in the two-chromophore case, namely, how alignment between chromophores results in complete correlation (at short times) between these two chromophores. For instance, if chromophores 1 and 2 are aligned, the correlation function is zero except when the $\boldsymbol{\omega}$ "vector" is perpendicular to vectors $(\mathbf{g}_2 \times \mathbf{g}_3)$ and $(\mathbf{g}_1 \times \mathbf{g}_3)$ at the same time, implying any of the ω_i's $(i = 1, 2, 3)$ is a linear combination of the other two.

Corrections to the Monopole Result in eq 16. Corrections to the monopole result in eq 16 can be estimated, for instance, by presenting the $\sum_\alpha J_{\alpha j}\xi_\alpha$ sum in eq 14 in a multipole-like expansion:[30]

$$\sum_\alpha J_{\alpha j}\xi_\alpha = -\mathbf{g}_j\nabla_j \sum_\alpha \xi_\alpha \mathbf{g}_\alpha \nabla_j \frac{1}{r_{\alpha j}} \simeq -\mathbf{g}_j\nabla_j \sum_\alpha \xi_\alpha \mathbf{g}_\alpha \nabla_j \left[\frac{1}{r_j} - (\mathbf{r}_{\alpha j} - \mathbf{r}_j)\frac{\mathbf{r}_j}{r_j^3}\right] \tag{24}$$

where $\mathbf{g}\nabla \equiv g_x\partial/\partial x + g_y\partial/\partial y + g_z\partial/\partial z$. The radius vector $\mathbf{r}_j$ connects spin j and the "center of mass" of the chromophore cluster. Here, we truncate the multipole expansion at the "dipole" term, which is linear in $(\mathbf{r}_{\alpha j} - \mathbf{r}_j)$. The first term in square brackets yields the lowest order result from eq 16. The

dx.doi.org/10.1021/jp401085p | J. Phys. Chem. B 2013, 117, 12734−12741

second term, after performing the derivatives, can be presented as $\sum_\alpha(\mathbf{r}_{\alpha j} - \mathbf{r}_j)\xi_\alpha \mathbf{A}_{\alpha j} r_j^{-4}$, where the vector $\mathbf{A}_{\alpha j}$ scales linearly with the product $g_j g_\alpha$ but does not depend on the vector $\mathbf{r}_\alpha$.

Next, in the usual fashion, we present the summation over the spins, $\sum_j B_j$ as integration in space over $\mathbf{r}_j$: $\sum_j \to n\int \mathrm{d}^3\mathbf{r}$, which assumes $\mathbf{r}_j$ is not correlated with $\mathbf{g}_j$ and γ_j. The latter integration can be performed in spherical coordinates, whereby the radial integration, at fixed values of the polar and azimuthal angle, has the form

$$\int_{r_{\min}}^{\infty} r_j^{\,2} B_j \left[\frac{c_1}{r_j^{\,3}} \left| \sum_\alpha \mathbf{g}_\alpha \xi_\alpha \right| + \frac{c_2}{r_j^{\,4}} \sum_\alpha (\mathbf{r}_{\alpha j} - \mathbf{r}_j)\xi_\alpha \mathbf{A}_{\alpha j} \right] \mathrm{d}r_j \tag{25}$$

where $c_1 > 0$ and c_2 are two constants whose precise value is not essential here. In addition, it is convenient to expand B_j to the lowest order in $(1 - f_j^2)$: $B_j(x) \simeq -2\gamma_{j\pm} t \sin^2(x)$, as appropriate at early times. This allows one to take the time dependence out of the integral, again, assuming $\mathbf{r}_j$ and γ_j are uncorrelated.

Let us first consider the case of two or three chromophores that are not strictly aligned. To evaluate the integral in eq 25, we change variables so that the expression in the square brackets is equal to x, while rescaling the radial variable r_j so that $c_1 = 1$ for convenience. At large values of $|\sum_\alpha \mathbf{g}_\alpha \xi_\alpha|$, as relevant for short times, the quantity $r_j^{\,3}$ can be expressed through x, using three leading terms in an expansion in terms of a small quantity $1/r_j^{\,3} \propto |\sum_\alpha \mathbf{g}_\alpha \xi_\alpha|$: $r_j^{\,3} \simeq (1/x)\{|\sum_\alpha \mathbf{g}_\alpha \xi_\alpha| + cx^{1/3}|\sum_\alpha \mathbf{g}_\alpha \xi_\alpha|^{-1/3}[\sum_\alpha(\mathbf{r}_{\alpha j} - \mathbf{r}_j)\xi_\alpha \mathbf{A}_{\alpha j}] - (c^2/3)x^{2/3}|\sum_\alpha \mathbf{g}_\alpha \xi_\alpha|^{-5/3}[\sum_\alpha(\mathbf{r}_{\alpha j} - \mathbf{r}_j)\xi_\alpha \mathbf{A}_{\alpha j}]^2\}$, where c is a numerical constant. This information is sufficient to take the integral (eq 25), in terms of the x variable, for each of the three terms above. The resulting three terms correspond to the monopole, dipole, and "dipole squared" term in the multipole expansion. Since the variables $(\sum_\alpha \mathbf{g}_\alpha \xi_\alpha)$ and $(\sum_\alpha(\mathbf{r}_{\alpha j} - \mathbf{r}_j)\xi_\alpha \mathbf{A}_{\alpha j})$ are generally linearly independent, the three terms scale, respectively, as $|\sum_\alpha \mathbf{g}_\alpha \xi_\alpha|$, $|\sum_\alpha \mathbf{g}_\alpha \xi_\alpha|^{2/3}$, and $|\sum_\alpha \mathbf{g}_\alpha \xi_\alpha|^{1/3}$ at large values of the latter. Finally, since at short times, the ξ integral in eq 13 is dominated by values $|\sum_\alpha \mathbf{g}_\alpha \xi_\alpha| \propto (\gamma t)^{-1}$ (as in the discussion preceding eq 11), it is easy to show that the dipole and dipole-squared corrections to the dominant, linear t dependence of the linewidth scale as $t^{4/3}$ and $t^{5/3}$, respectively. Although the former is *a priori* larger than the latter, it could be of either sign or even zero depending on the precise value of the total "dipole moment" of the chromophore set. In contrast, the "dipole squared" term is always non-zero and always leads to line *narrowing*. By an analogous argument, one can show that the next order, "quadrupole" term in the multipole expansion of the quantity results in a $t^{5/3}$ correction to the linewidth. Like the dipole term discussed above, the quadrupole correction could be of either sign or zero.

A more interesting situation arises when the leading, monopole term is strictly zero. The simplest realization of this situation is the limit of perfect alignment of two chromophores, whereby the "thickness" of the ridge in Figure 2, $\delta\omega_\perp$, would be zero. While the shape of the surface along the ridge is determined by the behavior of the broadening kernel B from eq 4, the shape across the bridge is determined by the conjugate variable $\xi_\perp = g_2\xi_1 - g_1\xi_2$, see eq 16. In the short-time, narrow line limit, it is the large $\xi_\perp$ asymptotics that determine the line shape across the ridge. In this limit, the dipole term from eq 25, which scales as $1/r^4$, becomes dominant. Considerations similar to the analysis of the multipole corrections above yield the following asymptotic form for the broadening kernel in the $\xi_\perp \to \infty$, $|\xi_\parallel| < \infty$ limit:

$$\sum_j B_j(\xi_\parallel, \xi_\perp) \sim -n\langle\gamma\rangle t\, |A\xi_\perp r_{12}|^{3/4} \tag{26}$$

up to a factor of order unity. The Fourier transform of the broadening kernel above is the so-called Levy (or "stable") law of index 3/4 (see, e.g., ref 31). (To give an example, the Lorentzian is the Levy law of index 1.) This function is rather close to the Lorentzian but differs from the latter at the wings. However, experimentally, the wings are not easily accessible and, at any rate, are dominated by various short wave length effects that we have neglected here. Of primary concern in the present context is the linewidth at the half-height, as pertinent to the Fourier image in eq 26. Dimensional considerations completely analogous to those leading to eq 11 yield eq 21.

The $\langle n\gamma\rangle$ Averaging. For the sake of simplicity, we will assume the tunneling barriers of the TLS in glasses are uniformly distributed, even though some weak corrections to this simple behavior are expected.[13] In a standard fashion, then, the combined distribution of total energy splitting E of a TLS and its relaxation rate γ is given by the expression[29]

$$n(E, \gamma) = \bar{P}\frac{\gamma^{-1}}{2\sqrt{1 - \gamma\tau_{\min}(E)}} \tag{27}$$

where the shortest relaxation time at energy E is computed according to[29]

$$\tau_{\min}^{-1} \simeq \frac{3g^2E^3}{2\pi\rho c_s^{\,5}} \coth(\beta E/2) \tag{28}$$

and we have neglected the difference between the speeds of longitudinal and transverse sound, both of which are denoted with c_s. In the equation above, ρ denotes the mass density and g is the coupling between phonons and the TLS.

As already mentioned, the averaging in eqs 10 and 22 is performed with respect to the parameters of individual TLS but also their initial configurations. Assuming the spins are in thermal equilibrium, the averaging over the initial configurations in eq 22 yields[8] $\langle n(E, \gamma)\gamma/2\cosh^2(\beta E/2)\rangle$, where the averaging is now only over the parameters of the TLS. Note that $\gamma_j/2\cosh^2(\beta E_j/2) = \gamma_{j,+}/(1 + e^{\beta E_j}) + \gamma_{j,-}/(1 + e^{\beta E_j})$ is the thermally averaged rate constant for flipping of spin j. Now, integrating $n(E, \gamma)\gamma/2\cosh^2(\beta E/2)$ over γ and E yields $\bar{P}(\pi^4/8)3g^2(k_BT)^3/2\pi\rho c_s^{\,5}$. We assume the typical TLS has a splitting that maximizes the expression for the heat capacity of a TLS, i.e., $(\beta E/2)^2/\cosh^2(\beta E/2)$: $E \simeq 2k_BT$: This indeed yields the simple estimate $\langle n\gamma\rangle \simeq \bar{P}T\tau^{-1}$, cited in the main text, where τ^{-1} denotes the value of the relaxation rate from eq 28 for the typical value of E.

AUTHOR INFORMATION

Corresponding Author

*E-mail: vas@uh.edu.

Notes

The authors declare no competing financial interest.

[§]Deceased.

ACKNOWLEDGMENTS

The authors thank Peter G. Wolynes for helpful comments. They gratefully acknowledge the NSF grant CHE 0306287 and the Donors of the Petroleum Research Fund of the American

Chemical Society. V.L.'s work is supported by NSF Grant CHE 0956127, Alfred P. Sloan Research Fellowship, and the Welch Foundation Grant No. E-1765.

REFERENCES

(1) Abragam, A. *The Principles of Nuclear Magnetism*; Oxford University Press: 1961.
(2) Mims, W. B. In *Electron Paramagnetic Resonance*; Geschwind, S., Ed.; Plenum Press: 1972; pp 263−351.
(3) Stoneham, A. M. Shapes of Inhomogeneously Broadened Resonance Lines in Solids. *Rev. Mod. Phys.* **1969**, *41*, 82.
(4) Klauder, J. R.; Anderson, P. W. Spectral Diffusion Decay in Spin Resonance Experiments. *Phys. Rev.* **1962**, *125*, 912−932.
(5) Black, J. L.; Halperin, B. I. Spectral Diffusion, Phonon Echoes, and Saturation Recovery in Glasses at Low Temperatures. *Phys. Rev. B* **1977**, *16*, 2879−2895.
(6) Boiron, A.-M.; Tamarat, P.; Lounis, B.; Brown, R.; Orrit, M. Are the Spectral Trails of Single Molecules Consistent with the Standard Two-Level System Model of Glasses at Low Temperatures? *Chem. Phys.* **1999**, *247*, 119−132.
(7) Bauer, M.; Kador, L. Electric-Field Effects of Two-Level Systems Observed with Single-Molecule Spectroscopy. *J. Chem. Phys.* **2003**, *118*, 9069−9072.
(8) Lubchenko, V.; Silbey, R. J. Spectral Diffusion and Drift: Single Chromophore and *en masse*. *J. Chem. Phys.* **2007**, *126*, 064701.
(9) Phillips, W. A., Ed. *Amorphous Solids: Low-Temperature Properties*; Springer-Verlag: Berlin, Heidelberg, New York, 1981.
(10) Anderson, P. W.; Halperin, B. I.; Varma, C. M. Anomalous Low-Temperature Thermal Properties of Glasses and Spin Glasses. *Philos. Mag.* **1972**, *25*, 1−9.
(11) Phillips, W. A. Tunneling States in Amorphous Solids. *J. Low Temp. Phys.* **1972**, *7*, 351.
(12) Lubchenko, V.; Wolynes, P. G. Intrinsic Quantum Excitations of Low Temperature Glasses. *Phys. Rev. Lett.* **2001**, *87*, 195901.
(13) Lubchenko, V.; Wolynes, P. G. The Microscopic Quantum Theory of Low Temperature Amorphous Solids. *Adv. Chem. Phys.* **2007**, *136*, 95−206.
(14) Lubchenko, V.; Wolynes, P. G. The Origin of the Boson Peak and Thermal Conductivity Plateau in Low Temperature Glasses. *Proc. Natl. Acad. Sci. U.S.A.* **2003**, *100*, 1515−1518.
(15) Lubchenko, V.; Silbey, R. J.; Wolynes, P. G. Electrodynamics of Amorphous Media at Low Temperatures. *Mol. Phys.* **2006**, *104*, 1325−1335.
(16) Zhugayevych, A.; Lubchenko, V. An Intrinsic Formation Mechanism for Midgap Electronic States in Semiconductor Glasses. *J. Chem. Phys.* **2010**, *132*, 044508.
(17) Zhugayevych, A.; Lubchenko, V. Electronic Structure and the Glass Transition in Pnictide and Chalcogenide Semiconductor Alloys. I: The Formation of the *ppσ*-Network. *J. Chem. Phys.* **2010**, *133*, 234503.
(18) Zhugayevych, A.; Lubchenko, V. Electronic Structure and the Glass Transition in Pnictide and Chalcogenide Semiconductor Alloys. II: The Intrinsic Electronic Midgap States. *J. Chem. Phys.* **2010**, *133*, 234504.
(19) Lubchenko, V.; Wolynes, P. G. Theory of Structural Glasses and Supercooled Liquids. *Annu. Rev. Phys. Chem.* **2007**, *58*, 235−266.
(20) Lubchenko, V. Quantum Phenomena in Structural Glasses: The Intrinsic Origin of Electronic and Cryogenic Anomalies. *J. Phys. Chem. Lett.* **2012**, *3*, 1−7.
(21) Yu, C. C.; Leggett, A. J. Low Temperature Properties of Amorphous Materials: Through a Glass Darkly. *Comments Condens. Matter Phys.* **1988**, *14*, 231.
(22) Neu, P.; Reichman, D. R.; Silbey, R. J. Spectral Diffusion on Ultralong Time Scales in Low-Temperature Glasses. *Phys. Rev. B* **1997**, *56*, 5250−5260.
(23) Esquinazi, P., Ed. *Tunneling Systems in Amorphous and Crystalline Solids*; Springer-Verlag: Heidelberg, 1998.
(24) Pohl, R. O.; Liu, X.; Thompson, E. Low-Temperature Thermal Conductivity and Acoustic Attenuation in Amorphous Solids. *Rev. Mod. Phys.* **2002**, *74*, 991−1013.
(25) Brown, F. L. H.; Silbey, R. J. An Investigation of the Effects of Two Level System Coupling on Single Molecule Lineshapes in Low Temperature Glasses. *J. Chem. Phys.* **1998**, *108*, 7434−7450.
(26) Bevzenko, D.; Lubchenko, V. Stress Distribution and the Fragility of Supercooled Melts. *J. Phys. Chem. B* **2009**, *113*, 16337−16345.
(27) Goubau, W. M.; Tait, R. A. Short-Time-Scale Measurement of the Low-Temperature Specific Heat of Polymethyl Methacrylate and Fused Silica. *Phys. Rev. Lett.* **1975**, *34*, 1220−1223.
(28) Lubchenko, V.; Wolynes, P. G. Barrier Softening near the Onset of Nonactivated Transport in Supercooled Liquids: Implications for Establishing Detailed Connection between Thermodynamic and Kinetic Anomalies in Supercooled Liquids. *J. Chem. Phys.* **2003**, *119*, 9088−9105.
(29) Jäckle, J. Ultrasonic Attenuation in Glasses at Low Temperatures. *Z. Phys.* **1972**, *257*, 212−223.
(30) Landau, L. D.; Lifshitz, E. M. *The Classical Theory of Fields*; Pergamon Press: 1979.
(31) Bouchaud, J.-P.; Georges, A. Anomalous Diffusion in Disordered Media - Statistical Mechanisms, Models, and Physical Applications. *Phys. Rep.* **1990**, *195*, 127−293.